Effect of Clotrimazole on the Pump Cycle of the Na,K-ATPase

Gianluca Bartolommei,* Nadège Devaux,[†] Francesco Tadini-Buoninsegni,* MariaRosa Moncelli,* and Hans-Jürgen Apell[†]

*Department of Chemistry, University of Florence, Florence, Italy; and [†]Department of Biology, University of Konstanz, Konstanz, Germany

ABSTRACT   The effect of the antimycotic drug clotrimazole (CLT) on the Na,K-ATPase was investigated using fluorescence and electrical measurements. The results obtained by steady-state fluorescence experiments with the electrochromic styryl dye RH421 were combined with those achieved by a pre-steady-state method based on fast solution exchange on a solid supported membrane that adsorbs the protein. Both techniques are suitable for monitoring the electrogenic steps of the pump cycle and are in general complementary, yielding distinct kinetic information. The experiments show clearly that CLT affects specific partial reactions of the pump cycle of the Na,K-ATPase with an affinity in the low micromolar range and in a reversible manner. All results can be consistently explained by proposing the CLT-promoted formation of an ion-occluded-CLT-bound conformational E_2 state, $E_2^{CLT}(X_2)$ that acts as a "dead-end" side track of the pump cycle, where X stands for H^+ or K^+. Na^+ binding, enzyme phosphorylation, and Na^+ transport were not affected by CLT, and at high CLT concentrations $\sim\frac{1}{3}$ of the enzyme remained active in the physiological transport mode. The presence of Na^+ and K^+ destabilized the inactivated form of the Na,K-ATPase.

INTRODUCTION

Clotrimazole (CLT) is an imidazole derivative that is usually employed as an antifungal agent (1). It has also been shown to inhibit cell proliferation (2,3) and to affect steroid metabolism (4) and sickle cell dehydration (5). At the molecular level these actions have been attributed to an inhibitory effect on cytochrome P-450 (6,7), SERCA pumps (8,9), and calcium-dependent K^+ channels (10–12). Moreover, thermosensory and chemosensory transient receptor potential channels in sensory neurons are targeted by this drug (13), as well as some multidrug resistance proteins (14,15). Interest in this chemical compound is increasing with respect to its potential antimalarial activity as a result of a rapid growth inhibition of different strains of the malaria parasite *Plasmodium falciparum* (16–18). For this reason, the chemical scaffold of CLT has been taken as a reference to develop new antimalarial agents to overcome *P. falciparum* resistance to currently available drugs (19). Although it is known that CLT can act on a large variety of targets, not much is known about the mechanisms of action.

This work further increases the range of potential targets of this drug because it provides experimental evidence that CLT is also an inhibitor of the Na,K-pump, a P-type ATPase that is essential for all mammalian cells. The Na,K-ATPase actively transports sodium and potassium ions against their electrochemical potentials across the plasma membrane of the cell by utilizing the free enthalpy of ATP hydrolysis (20,21).

The molecular mechanism of ion transport in P-type ATPases is usually described by means of the so-called Post-Albers cycle (22,23). According to this model, the pump can exist in two main conformations: E_1 and E_2 (Scheme 1 *A*). The E_1 conformation has a high affinity for sodium ions, can be phosphorylated by ATP, and presents the ion-binding sites to the cytoplasm. The E_2 conformation has a high affinity for potassium ions, can be phosphorylated by inorganic phosphate (P_i), and presents ion-binding sites to the extracellular aqueous phase. The recently determined crystallographic structure of the sodium pump (24) supports the concept that Na^+ and K^+ ions share common binding sites, with the exception of the third sodium ion, which binds to a distinct region.

To investigate the effect of CLT on the Na,K-pump, two different experimental techniques were employed in this work: a fluorescence technique that makes use of the electrochromic styryl dye RH421 (25,26), and a pre-steady-state electrical technique that is based on fast solution exchange on membrane fragments containing the Na,K-ATPase adsorbed to a solid supported membrane (SSM) (27,28). Both techniques can monitor electrogenic steps within the pump cycle of the protein. They are in general complementary, yielding distinct kinetic information, and have been applied in recent studies to identify and analyze the effect of various inhibitors on the reaction kinetics of Na,K-ATPase and SR Ca-ATPase (RH421 (29,30) and SSM (8,31,32)). The experiments reported in this work were carried out to investigate the CLT effect on different partial reactions of the pump cycle of the Na,K-ATPase. Our results reveal which partial reactions are affected by this compound and enable us to propose a molecular mechanism of the Na,K-pump inhibition by CLT.

MATERIALS AND METHODS

Materials

Magnesium, sodium and potassium chloride, tri-sodium citrate dihydrate, ammonium heptamolybdate tetrahydrate, potassium dihydrogen phosphate, 3-morpholinopropane sulfonic acid (MOPS), and tris(hydroxymethyl)-aminomethane (TRIS) were obtained from Merck (Whitehouse Station, NJ)
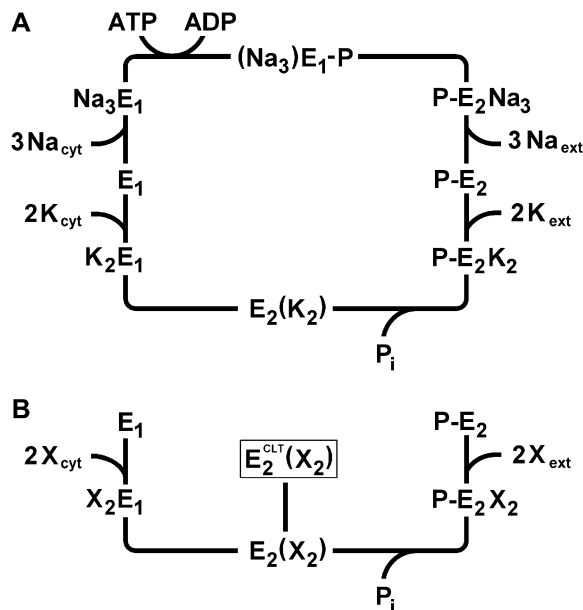
A

B

SCHEME 1 (*A*) Enzymatic cycle of Na,K-ATPase according to the Post-Albers model. Part *B* highlights the potassium branch of the cycle, indicating the proposed ion-occluded-CLT-bound state, $E_2^{CLT}(X_2)$. The *X* stands for a general cation (K^+ or H^+).

at analytical grade. Adenosine-5′-triphosphate disodium salt (ATP, ~97%), tween 20, TRIS phosphate (>99%), dithiothreitol (DTT, ≥99%), and ouabain were purchased from Fluka (Buchs, Switzerland). Phosphoenolpyruvate (PEP), pyruvate kinase/lactate dehydrogenase suspension (PK/LDH), β-nicotinamide adenine dinucleotide (reduced disodium salt hydrate, NADH), L-histidine, ethylenediaminetetraacetic acid (EDTA), malachite green hydrochloride, and 1-[o-chloro-α,α-diphenylbenzyl]-imidazole (CLT) were purchased from Sigma-Aldrich (St. Louis, MO) at the highest quality available. The electrochromic styryl dye RH421 was obtained from Molecular Probes (Eugene, OR).

Membrane preparation

Membrane fragments containing Na,K-ATPase were obtained by extraction from the outer medulla of rabbit kidneys using procedure C of Jørgensen (33). The enzyme activity of the Na,K-ATPase was determined by the PK/LDH method in a buffer containing 25 mM imidazole (pH 7.2), 100 mM NaCl, 10 mM KCl, 5 mM $MgCl_2$, 1.5 mM Na_2ATP, 2 mM PEP, 740 U/mL of pyruvate kinase (PK) and 931 U/mL lactate dehydrogenase (LDH), and initially 100 μM NADH. If the buffer lacks the presence of K^+ and ammonium ions, the Na-only mode activity can be measured (34). Control experiments were also performed under similar experimental conditions (100 mM NaCl, 20 mM KCl, 3 mM $MgCl_2$, 25 mM histidine, pH 7.2) with the colorimetric method based on malachite green developed by Lanzetta et al. (35) to exclude any effect of CLT on PK and/or LDH. Protein concentration was determined by the Lowry method using bovine serum albumin as a standard. The total protein content of membrane fragments was usually between 1.5 and 2.5 mg/mL, and specific ATPase activity was in the range of 1700–2100 μmol P_i/(h·mg protein) at 37°C. Enzyme activity could be completely blocked in the presence of 1 μM ouabain. Two different Na,K-ATPase preparations were used for all the experiments shown.

Fluorescence experiments with styryl dye RH421

The styryl dye RH421 is an amphiphilic molecule that dissolves in lipid membranes with a high partition coefficient ($\gamma_{lipid}/\gamma_{water} = 2.5 \times 10^5$ (26)).

The spectral changes of the styryl dye are predominantly due to an electrochromic effect: the energy difference between the ground state and the excited state depends on the presence of an electric field strength, and a modification of the electric field strength shifts the absorption band. In the presence of densely packed ion pumps such as Na,K-ATPase in purified membrane fragments, such a modification may arise from ion binding and translocations in the course of the pump cycle of the protein. As a consequence, the styryl dye responds with a shift of the absorption spectra to longer (red) or shorter (blue) wavelengths corresponding to changes in the local electric potential inside the membrane to more negative or more positive values, respectively (26).

Fluorescence measurements were performed by a JASCO FP-6500 spectrofluorometer. The excitation wavelength was set to 580 nm (slit width = 10 nm) and the emission wavelength was set to 650 nm (slit width = 20 nm). A high-pass optical filter ($\lambda_{cut} = 590 \pm 6$ nm; Edmund Optics, Barrington, NJ) was put between the cuvette and the detector to cut off contributions to the emitted radiation due to higher harmonics. The temperature in the permanently stirred quartz semimicrocuvette (0.7 mL, 109.004F-QS; Hellma, Müllheim, Germany) was maintained at 20°C by a water thermostat. Under these conditions the required reagents were added to the buffer solution into the cuvette, and at the same time the fluorescence emission by the RH421 dye was recorded.

The standard buffer solution contained 25 mM histidine (pH 7.2), 0.5 mM EDTA, and 5 mM $MgCl_2$, pH 7.2. After an equilibration time of 10 min, the styryl dye RH421 was added to the main buffer solution from a 200 μM ethanolic stock solution to obtain a final concentration of 200 nM. After 5 min, an aqueous suspension of membrane fragments containing the Na,K-ATPase was added. The final protein concentration was in the range of 8–11 μg/mL. Subsequent aliquots added to the cuvette depended on the experimental conditions. Aliquots of NaCl, KCl, ATP, or inorganic phosphate (P_i) were added from concentrated stock solutions. Ouabain was added from a 5-mM stock solution in water, and CLT was added from a 2.5-mM solution in dimethyl sulfoxide (DMSO). When needed, higher-diluted stocks were prepared.

Data obtained from each fluorescence experiment were stored in arbitrary units and normalized according to the function $\Delta F/F_0 = (F - F_0)/F_0$, with respect to the initial fluorescence level before the first substrate addition, F_0, so that different experiments could be compared easily.

Pre-steady-state electrical measurements

Pre-steady-state electrical measurements were carried out with the rapid concentration jump method developed by Pintschovius and Fendler (27). Membrane fragments containing the protein were adsorbed onto a surface-modified gold electrode (the SSM) and perturbed by a fast concentration jump of an appropriate substrate. If at least one electrogenic step is involved in the relaxation process after the perturbation, a current transient can be observed. The multiexponential fitting of the transient provides kinetic information regarding the reaction steps involved in the relaxation process, whereas the translocated charge is obtained by integration of the peak current. Further experimental details can be found in Pintschovius and Fendler (27) and Tadini-Buoninsegni et al. (28,36).

In general, a washing (i.e., nonactivating) solution and an activating solution were employed: the washing solution contained 130 mM NaCl, 25 mM MOPS (pH 7.0), 3 mM $MgCl_2$, and 0.2 mM DTT. The activating solution had the same composition as the washing solution plus ATP 100 μM. When present, CLT was added to both solutions at the required concentration.

All measurements were carried out using the $SURFE^2R^{One}$ device (Ion-Gate Biosciences, Frankfurt, Germany) (37).

RESULTS

Reduction of enzyme activity

The first evidence of an effect of CLT on the Na,K-ATPase was that the antimycotic drug reduced ATP hydrolysis to as

much as 35–40% of the initial value at high CLT concentrations (100 μM) in the presence of Na^+ and K^+. In the absence of KCl (i.e., in the Na-only mode), the residual hydrolytic activity at high CLT concentrations was reduced to ~22% of the initial value. Measurements were performed extensively by means of the coupled-enzymes assay and, as a control, the colorimetric method to exclude any effect of CLT on the coupled-enzymes assay (Fig. 1).

The dependence of the enzyme activity on the CLT concentration was characterized by the parameters of the Hill function used to fit the experimental data. In the presence of NaCl and KCl, a good agreement of the parameters was obtained for both experimental methods. In particular, from the coupled enzymes assay a half-saturation constant, $K_{0.5}$, of 24 ± 1 μM, and a coefficient of cooperativity, n, of 3.2 ± 0.4 were obtained (Fig. 1, *solid circles* and *solid line*), whereas the colorimetric test provided values of $K_{0.5} = 30 \pm 4$ μM and $n = 2.9 \pm 1.7$ (Fig. 1, *open circles* and *dotted line*). In the Na-only mode, the half-saturation constant was significantly lower ($K_{0.5} = 9.5 \pm 1.1$ μM), whereas the coefficient of cooperativity was practically unchanged ($n = 2.3 \pm 0.6$; Fig. 1, *solid squares* and *dotted line*). In all three cases, a coefficient of cooperativity >1 appears to indicate that more than one molecule of CLT binds to affect enzyme activity. The half-saturation constant on the order of 10–30 μM entitled us to define CLT as a medium-affinity inhibitor of the Na,K-ATPase.

These experiments clearly show that CLT decreased the enzymatic activity of the sodium pump. The notable reduction of its ATP-hydrolytic activity at high CLT concentra-

FIGURE 1 ATPase hydrolytic activity of Na,K-ATPase in the presence of NaCl and KCl ($\bullet$,$\circ$) or NaCl only (Na-only mode, $\blacksquare$). The activities were determined by means of the PK/LDH ($\bullet$,$\blacksquare$) and malachite green ($\circ$) methods in the presence of increasing concentrations of CLT. The lines represent the best fittings by a Hill function. In the presence of NaCl and KCl the fitting gives $K_{0.5} = 24 \pm 1$ μM and $n = 3.2 \pm 0.4$ for the PK/LDH method (*solid line*), and $K_{0.5} = 30 \pm 4$ μM and $n = 2.9 \pm 1.7$ for the malachite green test (*dashed line*). The residual activity at high CLT concentration is 0.34 ± 0.02 and 0.39 ± 0.06, respectively. In the Na-only mode $K_{0.5}$ and n values are 9.5 ± 1.1 μM and 2.3 ± 0.6, respectively, whereas the residual activity is 0.22 ± 0.05 (*dotted line*). All data are normalized with respect to the activity in the absence of the drug.

tions may have, in principle, two different origins: 1), when CLT is bound, the rate constant of a step in the pump cycle is reduced so much that it produces the observed turnover rate; or 2), there is a complete inhibition of the pump in one (or more) states of the pump cycle. In the latter case, the remaining enzyme activity even at high concentrations would indicate that CLT binds reversibly to the protein.

Fluorescence measurements

Preliminary observations

Steady-state fluorescence measurements were performed with the electrochromic styryl dye RH421. In the basic experiment (the so-called standard experiment), Na,K-ATPase-containing membrane fragments (9 μg/mL protein) and 200 nM RH421 were equilibrated in standard buffer before 50 mM NaCl, 500 μM ATP, and 20 mM KCl were added successively from respective stock solutions. A typical time course of the obtained fluorescence trace is shown in Fig. 2 *A*, and it is in agreement with data from the literature (29,38,39).

At pH 7.2 and in the absence of either Na^+ or K^+, the protein assumes a proton-bound conformation, H_xE_1 with $1 < x < 2$ (level 1 in Fig. 2), which is quantitatively shifted to Na_3E_1 (level 2) after the addition of saturating Na^+. Subsequent addition of 500 μM ATP triggers sodium occlusion, protein phosphorylation, conformational change from E_1 to E_2, and sodium release on the extracellular side. The release of sodium ions decreases the amount of positive charge inside the protein, thus inducing a fluorescence increase (level 3, P-E_2). The final addition of 20 mM K^+ promotes the protein into the turnover condition, accompanied by a fluorescence decrease due to a positive charge accumulation inside the membrane. In this case the corresponding fluorescence level (number 4) is due to the weighted contribution of the ion-occluded conformations P-$E_1(Na_3)$ and $E_2(K_2)$. This can be recognized by a fluorescence level close to that of the state $(Na_3)E_1$-P (Fig. 2 *A*).

The fluorescence decrease observed after the addition of saturating Na^+ concentrations to the protein should be ~⅓ of the fluorescence increase obtained with the ATP addition to state Na_3E_1. This is explained by the fact that only the third sodium ion is bound electrogenically, whereas at pH 7.2 the first two Na^+ ions are exchanged electroneutrally against two H^+ ions in the binding sites. After the conformation transition, $Na_3E_1 \rightarrow$ P-E_2Na_3, all three sodium ions are released electrogenically from the protein, producing a charge movement ~3 times greater than that of the cytoplasmic sodium binding (38,40). When saturating KCl concentrations are added, the pump experiences turnover conditions and the resulting fluorescence level is controlled by the ion-occluded conformations (see above).

To analyze CLT effects on the sodium pump in terms of single reaction steps of the pump cycle, several series of experiments were carried out. First of all, CLT was added to
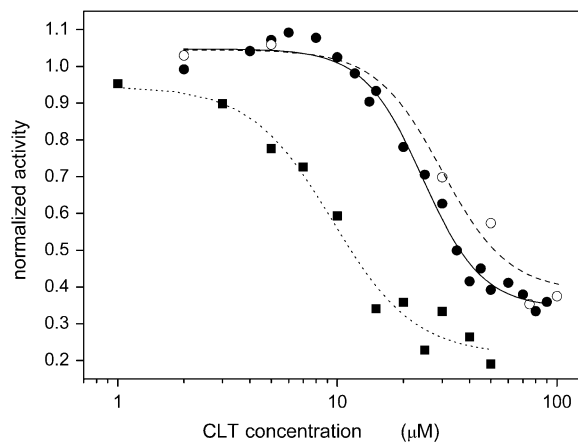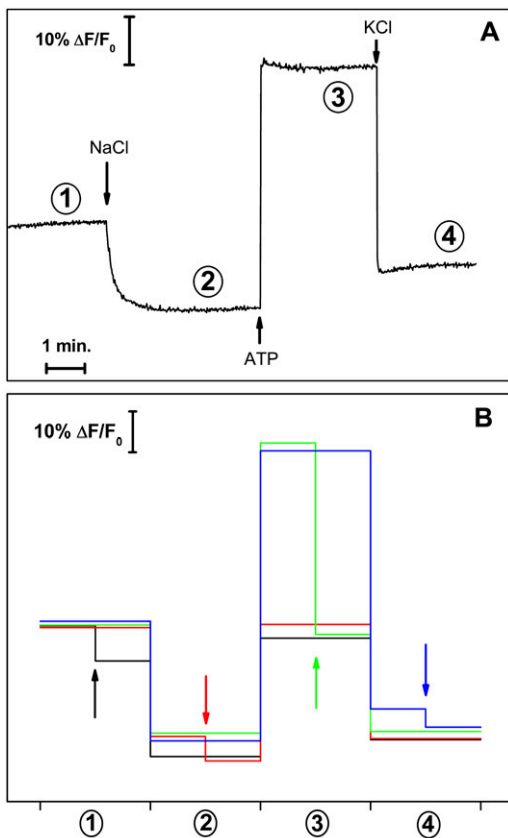
FIGURE 2 Fluorescence changes observed in the standard experiments. (*A*) The experimental trace represents the fluorescence emission of the RH421 dye at 660 nm for subsequent additions of 50 mM NaCl, 0.5 mM ATP, and 20 mM KCl to the standard buffer. Each steady-state fluorescence level is related to the preferentially adopted conformation for the experimental conditions employed: 1), H_xE_1 ($1 \leq x \leq 2$; in this preparation x can be estimated to be 1.8); 2), Na_3E_1; 3), $P\text{-}E_2$; and 4), $E_2(K_2)+P\text{-}E_1(Na_3)$. (*B*) Four different overlaid standard experiments are indicated by different colors. In each experiment an addition of 25 μM CLT was made at a different state of the standard experiment as indicated by the arrows in the corresponding color.

the protein in each one of the four steady-state fluorescence levels achieved in the course of four different standard experiments (Fig. 2 *B*). These experiments reveal the sensitivity of the protein for CLT in the states available under the respective substrate conditions. The addition of 25 μM CLT shows a clear reduction of the normalized fluorescence level in the case of the H_xE_1 ($x \approx 1.8$; see below) and $P\text{-}E_2$ states, whereas the fluorescence in states are less affected in the states of $Na_3 E_1$ and $E_2 (K_2)$, because the ion-binding sites are fully occupied by 3 Na^+ or 2 K^+. Moreover, the steady-state fluorescence levels attained by the ion pump after the addition of CLT (*arrows* in Fig. 2 *B*) are the same independently of the state at which CLT was added (Fig. 2 *B*). This fact indicates that CLT does not block progress through the pump cycle of the Na,K-ATPase in one of the transient states, H_2E_1, Na_3E_1, and $P\text{-}E_2$.

Control experiments

To clarify whether the observed fluorescence decreases are due to a specific interaction of CLT with the Na,K-ATPase or to a direct interaction with the RH421 molecules, CLT titrations were performed under three conditions in which the Na,K-ATPase was confined to a single defined state, as shown in Fig. 3. In these experiments aliquots of 5 μM CLT were added up to a final concentration of 50 μM. In the first experiment 50 mM NaCl were added before the CLT titration to generate quantitatively the state Na_3E_1, which has the lowest fluorescence level in the whole cycle as a result of the three positive charges in the binding sites. The subsequent additions of CLT (Fig. 3, *solid circles*) show an initial fluorescence decrease of $\sim$5% with a minimum at 10 μM CLT and a subsequent increase to approximately the initial level at 25 μM and above. A similar behavior was found in the presence of 20 mM KCl, a condition in which the pumps are trapped quantitatively in the occluded state $E_2(K_2)$ (Fig. 3, *solid triangles*). The third control experiment was performed when the Na,K-ATPase was completely inhibited by 100 μM ouabain in the presence of Na^+ and ATP. It has been shown that ouabain preferentially binds to the $P\text{-}E_2(Na_2)$ state of the enzyme and forms a completely inhibited ion pump (41). Again, a similar pattern in the CLT-dependent fluorescence change was detected (Fig. 3, *open squares*), an initial fluorescence decrease of $\sim$6% at 10–15 μM was followed by an almost complete reversal at 30 μM CLT. The last set of controls was performed in artificial lipid vesicles made from dioleoyl lecithin. A vesicle suspension was equilibrated in standard buffer ($\sim$13 μg lipid /mL) with 200 nM RH421 and
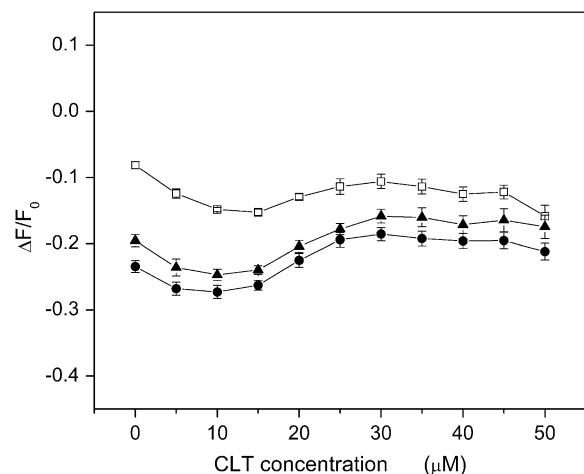

FIGURE 3 Fluorescence changes after subsequent CLT additions to the Na,K-ATPase corresponding to different steady-state fluorescence levels of the standard experiment in the absence ($\bullet$, $\blacktriangle$) or presence ($\square$) of 100 μM ouabain: after Na^+ addition ($\bullet$), after K^+ addition ($\blacktriangle$), and after ATP addition ($\square$). In the last titration (i.e., in the presence of ouabain) the protein is in a totally inhibited state and any fluorescence variation is only correlated with a nonspecific interaction of CLT with the dye in the lipid environment (artifact). Experiments were performed in standard buffer.

with or without 50 mM NaCl. After a stable fluorescence signal was obtained, CLT titration was performed in a manner similar to that described above. In these experiments also a small fluorescence decrease was detected with a minimum at ~10 μM CLT and a reversal of this effect at 25 μM (data not shown).

In summary, these minor fluorescence effects may be interpreted as an unspecific effect of CLT on the RH421 fluorescence. If, however, experiments are performed in the presence of 25 μM CLT, this artifact may be neglected.

Another feature of the CLT titrations is that the unspecific effect varied among the different protein preparations used. In particular, the minimum fluorescence level could be found at different concentrations of CLT between 10 μM and 20 μM, although in any case the minimal fluorescence level of the unspecific effect was in the range of 5–10%. This behavior may be assigned to the hydrophobic nature of CLT. Because of the significant partition coefficient of CLT between the lipid and aqueous phases, slight variations in the lipid composition and the protein density in the membrane, as found in different preparations, may modify the partition equilibrium and thus control the unspecific effect. On the other hand, the specific effects of CLT on the pump protein, like those discussed below, were in good agreement for the different preparations used (not shown).

With all this in mind, more detailed investigations of each steady-state fluorescence level were carried out.

Na$^+$ titrations

To study the effect of CLT on the sodium-binding kinetics in the E$_1$ conformation of the Na,K-ATPase, NaCl titrations were performed in the presence of different concentrations of CLT starting from the H$_2$E$_1$ level, H$_2$E$_1$ + 3 Na$^+$ $\rightarrow$ Na$_3$E$_1$ + 2 H$^+$. Na,K-ATPase-containing membrane fragments (9 μg/mL protein) and 200 nM RH421 were equilibrated in standard buffer. When a stable fluorescence level was reached, 0–25 μM CLT were applied before aliquots of NaCl were added up to a concentration of 200 mM. Results are shown in Fig. 4. The data points obtained from the fluorescence levels taken after each addition of Na$^+$ can be fitted satisfactorily by the following Hill function (Fig. 4 A):

$$\Delta F/F_0 = (\Delta F/F_0)_0 + (\Delta F/F_0)_{max} \left[\frac{c^n}{c^n + K_{0.5}^n} \right]. \quad (1)$$

$(\Delta F/F_0)_0$ is the initial fluorescence level at 0 Na$^+$, $(\Delta F/F_0)_{max}$ is the maximum fluorescence change attained at saturating Na$^+$ concentrations, c is the Na$^+$ concentration, $K_{0.5}$ is the half-saturation concentration, and n is the Hill coefficient, related to the cooperativity of the substrate binding process. The dependence of $K_{0.5}$ and n on CLT concentration was determined from the experimental data and is shown in Fig. 4, B and C, respectively. Neither one is significantly affected by CLT. The half-saturation constant remains practically unmodified at an average value $K_{0.5} = 7.3 \pm 0.6$ mM, and the
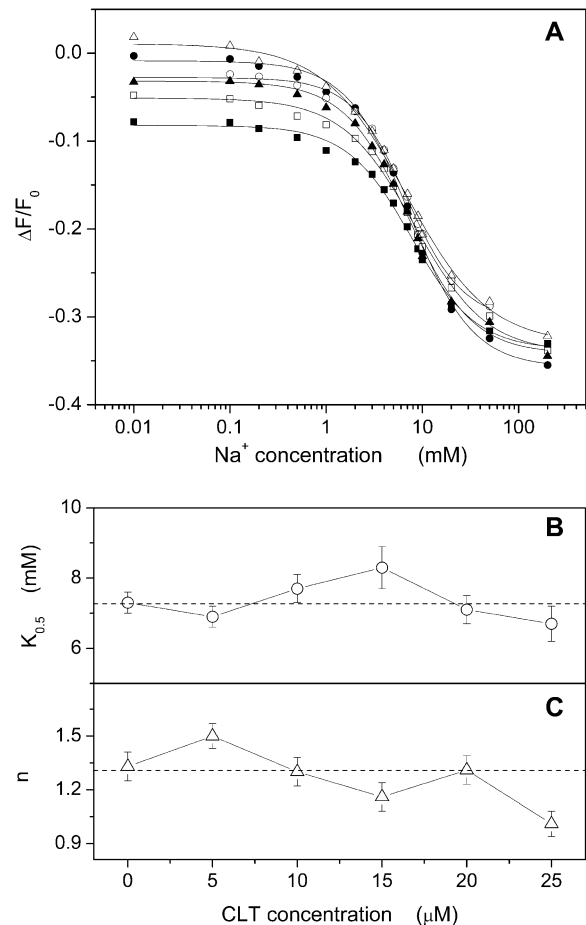

FIGURE 4 (A) Fluorescence changes correlated with titrations of the Na,K-ATPase by Na$^+$ ions in standard buffer at different CLT concentrations: 0 (●), 5 (○), 10 (■), 15 (□), 20 (▲), and 25 (△) μM. For each titration the relative fitting curve obtained by a Hill function is shown. Panels B and C show the dependence on CLT concentration of the half-saturation constant and the Hill coefficient, respectively, for each fitting curve. Dotted lines mark the averaged values: 7.3 ± 0.6 mM for $K_{0.5}$ and 1.3 ± 0.2 for n.

same is true for the Hill coefficient (average value $n = 1.3 \pm 0.2$). At 200 mM NaCl the fluorescence levels tend to merge within a variation of ~5% (Fig. 4 A), in agreement with the CLT-dependent artifact found at saturating Na$^+$ in Fig. 3 (solid circles). At low Na$^+$ concentrations the CLT-induced effect on the fluorescence is more pronounced; aside from the unspecific artifact, it consists of a CLT-induced modification of the ion pump (see below).

K$^+$ titrations

Similar titrations were carried out to analyze the potassium-binding kinetics in the P-E$_2$ conformation of the Na,K-ATPase, P-E$_2$ + 2 K$^+$ $\rightarrow$ E$_2$(K$_2$), in the presence of different CLT concentrations. The P-E$_2$ conformation was maintained by equilibrating the membrane fragments in standard buffer with 50 mM NaCl and 0.5 mM Na$_2$ATP, pH 7.0. This state can be identified by the highest fluorescence level detected in

the standard experiment (Fig. 2 *A*). In the absence or presence of up to 25 μM CLT, KCl was added in small aliquots to titrate K$^+$ binding sites until saturation at 20 mM. The results from these experiments are shown in Fig. 5. The data points obtained from the fluorescence levels taken after each addition of K$^+$ can be also fitted satisfactorily by the Hill function (Eq. 1) as shown in Fig. 5 *A*.

In contrast to the Na$^+$ titration experiments, a more significant effect of CLT is reflected in the concentration dependence of the fitting parameters. In particular, the half-saturation concentration increased monotonically by a factor of 2 (Fig. 5 *B*) from 0.32 $\pm$ 0.01 mM (0 CLT) to 0.65 $\pm$ 0.02 mM (25 μM CLT). This rise of $K_{0.5}$ indicates an apparent reduction of the affinity of the binding sites for K$^+$ ions. The Hill coefficient gradually decreased from an initial value of 1.28 $\pm$ 0.06 to a final value of 1.02 $\pm$ 0.03 (Fig. 5 *C*). Taking into account the CLT-induced artifact, the titration curves tend to merge at saturating potassium concentration at a fluores-
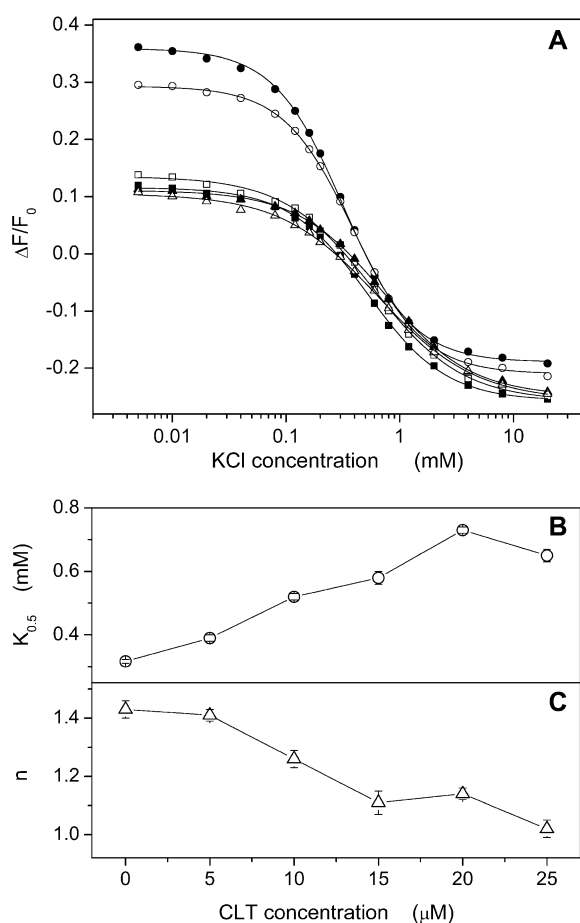

FIGURE 5 (*A*) Fluorescence changes due to K$^+$ titration of the Na,K-ATPase in standard buffer with 50 mM NaCl and 0.5 mM ATP at different CLT concentrations: 0 (●), 5 (○), 10 (■), 15 (□), 20 (▲) and 25 (△) μM. For each titration the relative fitting curve obtained by a Hill function is shown. Panels *B* and *C* show the dependence on CLT concentration of the half-saturation constant and the Hill coefficient, respectively, for each fitting curve.

cence level slightly above the level of the Na$_3$E$_1$ state, which is typical for the Na,K-ATPase under turnover conditions.

P$_i$ titrations by backdoor phosphorylation

The Na,K-ATPase can be phosphorylated by inorganic phosphate (P$_i$) in the absence of both Na$^+$ and K$^+$ ions, but the presence of Mg^{2+} is required. The reaction is known as ''backdoor phosphorylation,'' and in principle can be split into two reaction steps. In the first step, the enzyme undergoes a conformation transition, H$_2$E$_1$ $\rightarrow$ E$_2$(H$_2$), and in the second step the actual phosphorylation occurs, E$_2$(H$_2$) + P$_i$ $\rightarrow$ P-E$_2$H$_2$ (42). In the absence of Na$^+$ and K$^+$, H$^+$ acts as congeneric ion species since the formation of the occluded state with empty binding sites, E$_2$(), is energetically unfavorable. The electrogenicity of the backdoor phosphorylation is due to the release of both H$^+$ in the P-E$_2$ conformation, P-E$_2$H$_2$ $\rightarrow$ P-E$_2$, since the proton-binding affinity in the P-E$_2$ conformation is significantly lower than in the E$_1$ conformation (38). At pH 7 and high phosphate concentrations ($>$500 μM), the fluorescence increase observed upon backdoor phosphorylation represents an almost complete electrogenic proton release from the binding sites to the extracellular aqueous phase (42). Considering that phosphorylation from ATP or P$_i$ results in chemically identical phosphoenzymes, backdoor phosphorylation represents the reversal of the hydrolysis step of the P-E$_2$ state in the pump cycle under physiological conditions.

To perform backdoor phosphorylation experiments, Na,K-ATPase-containing membrane fragments were equilibrated in standard buffer with 200 nM RH421 until a constant fluorescence level was obtained. Then, TRIS phosphate (pH 7.2) was added in appropriate aliquots up to 1 mM to titrate the pump into its phosphorylated state. The respective fluorescence levels were plotted against the phosphate concentration as shown in Fig. 6 *A* (*solid circles*). This kind of experiment was repeated in the presence of up to 20 μM CLT. The concentration dependence of the fluorescence was fitted by the Hill function (Eq. 1), and the characteristic parameters, $K_{0.5}$ and *n*, were plotted against the CLT concentration (Fig. 6, *B* and *C*).

In the absence of CLT the half-saturation constant for P$_i$ was found to be 16.1 $\pm$ 0.8 μM (Fig. 6 *B*). This value decreased to 10 μM when CLT was increased to 15 μM. (The almost vanishing fluorescence change in the presence of 20 μM CLT relativizes the relevance of the low $K_{0.5}$ value at 20 μM CLT.) This behavior indicates an apparent increasing affinity of the sodium pump for P$_i$, and thus excludes a competition between P$_i$ and CLT binding to the protein. The Hill coefficient of enzyme phosphorylation is 1.0 $\pm$ 0.1 and is independent of the CLT concentration (Fig. 6 *C*).

The fluorescence level in the absence of CLT and at saturating P$_i$ concentrations corresponds to that of the state P-E$_2$. It is clearly affected by the presence of the drug. The fluorescence level upon addition of P$_i$ is practically unchanged in
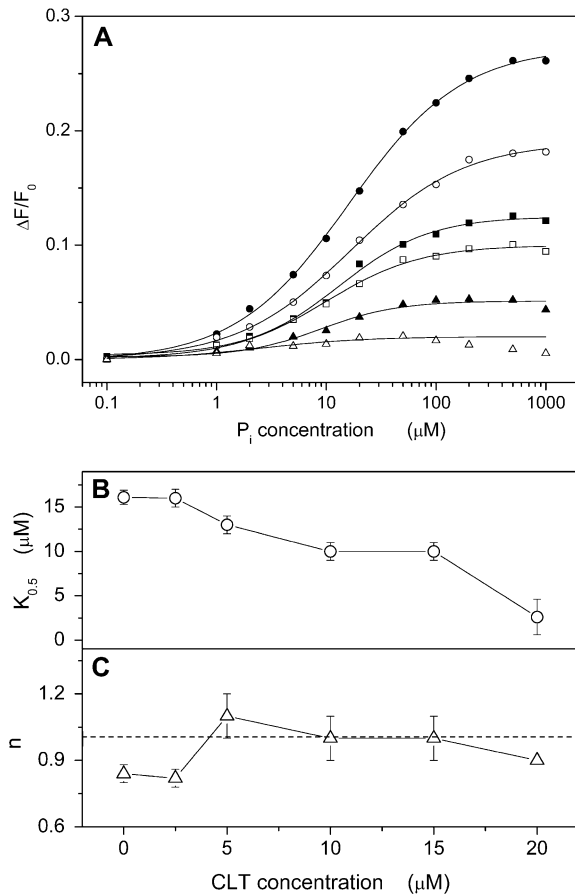
FIGURE 6 (*A*) Fluorescence changes associated with titration of the Na,K-ATPase in standard buffer by inorganic phosphate (P_i) at different CLT concentrations: 0 (●), 2.5 (○), 5 (■), 10 (□), 15 (▲), and 20 (△) μM. For each titration the relative fitting curve obtained by a Hill function is shown. Panels *B* and *C* show the dependence on CLT concentration of the half-saturation constant and the Hill coefficient, respectively, for each fitting curve. The dotted line in panel *C* marks the averaged value for *n* (1.0 ± 0.1).

the presence of 20 μM CLT. This observation indicates that CLT interaction with the Na,K-ATPase prevents the release of H^+, which requires the transition into the $P\text{-}E_2$ state.

pH titrations

The last series of fluorescence measurements were pH titrations in the absence and presence of 25 μM CLT. Supplying protons to the Na,K-ATPase in the absence of Na^+ and K^+ induces a right shift in the reaction sequence, $H_xE_1 \rightarrow H_2E_1 \rightarrow E_2(H_2)$. At pH 7.2 the value of *x* is on the order of 1.5–1.8, depending on the variation between different enzyme preparations. The experiments were performed in standard buffer in which 200 nM RH421 and membrane fragments (11 μg/mL protein) were equilibrated at pH 7.2. Without or after the addition of 25 μM CLT, pH titrations were carried out by addition of small aliquots of 1M HCl. The fluorescence changes were normalized with respect to the level before the first addition. Electrolyte pH was controlled by a pH micro-
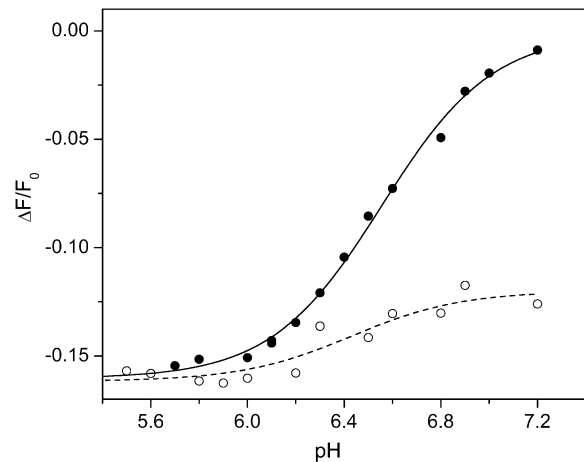

FIGURE 7 Fluorescence changes accompanying pH titration of Na,K-ATPase in standard buffer in the absence (●) and presence (○) of 25 μM CLT. Drawn lines represent fitting curves of the experimental data by a Hill function: pK = 6.56 ± 0.02 and *n* = 1.9 ± 0.2 (*solid line*); pK = 6.4 ± 0.1 and *n* = 1.9 (*dotted line*).

electrode. The steady-state fluorescence level after each addition of HCl was plotted against the respective pH (Fig. 7).

The experimental data could be fitted satisfactorily with the Hill function (Eq. 1). In both cases the Hill coefficient, *n*, was ~1.9, indicating cooperative proton binding. The half-saturating proton concentrations, determined as pK, were 6.56 ± 0.02 (0 CLT) and 6.4 ± 0.1 (25 μM CLT), and did not differ appreciably, although the fluorescence change was significantly reduced in the presence of CLT by a factor of ~4. At low pH, the fluorescence levels of both experiments merged. This fact allows us to exclude the possibility that the initial fluorescence decrease upon CLT addition may be attributed to the CLT-induced fluorescence artifact reported in Fig. 3.

Electrical measurements

Since the RH421 experiments provide insight into the interference of CLT with substrate-binding and release reactions of the pump cycle, a study of the ATP-driven conformation transition from the E_1 to the $P\text{-}E_2$ conformation was also desirable. To complete the investigations of the CLT interactions with the Na,K-ATPase, pre-steady-state electrical measurements were carried out by employing rapid-flow ATP exchanges onto an SSM with adsorbed membrane fragments. The experiments were performed with various CLT concentrations between 0 and 30 μM as described in the Materials and Methods section.

Two of these experiments, in the absence and presence of 25 μM CLT, are presented in Fig. 8. The numerical integration of the current transients yields the amount of charge, *Q*, translocated during the relaxation process that follows protein activation. To be able to compare the experiments at various CLT concentrations, the charge before and after addition of CLT were set in relation by $Q_{\text{normalized}} = Q_{+\text{CLT}}/Q_{-\text{CLT}}$. Since
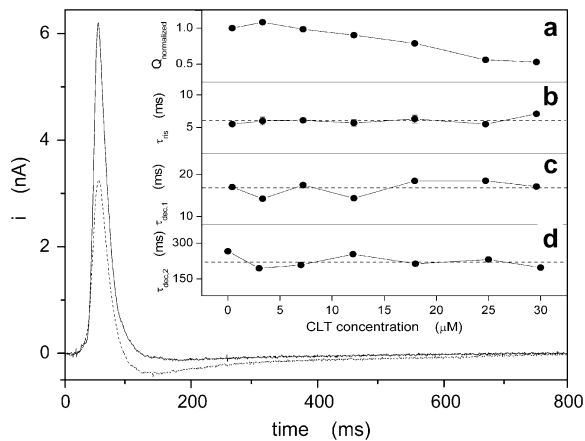
FIGURE 8 Experimental current transients obtained after a 100 μM ATP concentration jump in the absence (*solid line*) or presence (*dotted line*) of 25 μM CLT. The inset shows the dependence of the normalized charge (*a*) and time constants (*b*, rising phase; *c* and *d*, decay phase) on CLT concentration. Dashed lines indicate averaged values for the time constants: (*b*) 6.0 $\pm$ 0.6 ms; (*c*) 17 $\pm$ 2 ms; and (*d*) 224 $\pm$ 28 ms.

the ATP-concentration jumps were performed in the presence of sodium ions, the initial conformation was Na_3E_1 (Scheme 1 *A*), and the current measured was mainly due to sodium release to the extracellular side. Since K^+ was absent, only the Na^+-branch of the pump cycle contributed to the detected currents in the time course of these experiments (27). On the other hand, ion binding and/or release from the sodium pump are known to be very fast processes (43,44), and are not resolved kinetically with this method. Therefore, the time constants obtained by fitting of experimental transients are related to the rate-limiting steps preceding the electrogenic event. In our case, these detected steps are protein phosphorylation ($Na_3E_1 \rightarrow (Na_3)E_1$-P) and the subsequent transition into the P-E_2 conformation, $(Na_3)E_1$-P $\rightarrow$ P-E_2Na_3. The time course of the current transient can be fitted by the sum of three exponential functions: one rising and two falling. The respective time constants, τ_{ris} and $\tau_{dec,1}$, may be used to characterize partial reactions of the pump cycle, whereas the second time constant of the decreasing phase, $\tau_{dec,2}$, can be interpreted as the time constant of the discharging capacitance of the compound membrane (27). The values obtained experimentally in the absence of CLT are in very good agreement with those reported by Pintschovius and Fendler (27).

Fig. 8 demonstrates that the presence of 25 μM CLT significantly reduced the current transient. The systematic analysis of the dependence of this effect on CLT concentration is documented in the insets of Fig. 8. The ATP-induced Na^+ transport in terms of translocated charge, $Q_{normalized}$, decreased linearly with CLT concentration to $\sim$50% at 30 μM (inset *a*). In contrast, the time constants, τ_{ris} and $\tau_{dec,1}$, which are related to the kinetics of the Na^+ transport by the Na,K-ATPase, are independent of the CLT concentration

(insets *b* and *c*) as is $\tau_{dec,2}$, which reflects an electrical feature of the measuring system rather than a property of the ion pumps (inset *d*).

All of this experimental evidence shows that CLT does not interfere with the kinetics of the ATP binding and the subsequent Na^+ transport, $Na_3E_1 \rightarrow Na_3E_1ATP \rightarrow (Na_3)E_1$-P $\rightarrow$ P-$E_2Na_3 \rightarrow$ P-E_2. In addition, the presence of CLT does not even perturb the electrical properties of the compound membrane.

DISCUSSION

As shown in Fig. 1, the enzyme activity of the sodium pump can be progressively inhibited by the addition of increasing concentrations of CLT. It is noteworthy to mention that even at the highest CLT concentrations applied, the residual enzyme activity is $\sim$⅓ of the value in the absence of the drug in the physiological mode and $\sim$20% in the Na-only mode. This result is a clear indication that the interaction of CLT with the protein must be reversible in competition with other reaction steps of the pump cycle. The half-inhibiting CLT concentration of $K_{0.5} = 24$–30 μM is comparable to the inhibiting effects on the SR Ca-ATPase (8). This similarity in the functional modification by CLT and the close structural similarity of both ion pumps indicate a comparable inhibition mechanism.

Concerning the experiments at high CLT concentrations, it should be noted that aqueous CLT solutions at concentrations >30 μM became opalescent because of the high hydrophobicity of CLT, which makes it only poorly soluble in water, and formation of CLT micelles or adsorption of CLT to the surface of the membrane fragments may occur. Therefore, we cannot be sure that in the presence of high CLT concentrations the actual concentration affecting the protein is equal to the nominal concentration.

The enzyme activity of the Na,K-ATPase is an overall parameter of pump function and does not allow one to discriminate between affected and unaffected steps in the pump cycle of the protein (Scheme 1 *A*) when a CLT-induced reduction occurs. The evident reduction of Na,K-ATPase hydrolytic activity demonstrates, however, that CLT interacts in some way with the sodium pump. Two different experimental methods were applied in recent studies to identify and analyze the effect of inhibitors on the reaction kinetics of Na,K-ATPase and SR Ca-ATPase. In some studies, the fluorescent, electrochromic styryl dye RH421 was used to detect ion binding and release in the ion pump, as well as the effects of pump-inhibiting drugs (29,30). In other studies, pre-steady-state electrical measurements were utilized to detect ATP-induced charge movements in membrane fragments adsorbed to SSMs (8,31,32). The experiments presented above were performed with both methods, which allowed us to cover the different partial reactions of the pump cycle shown in Scheme 1 *A*. They revealed the affected

partial reactions and provided a confinement of possible inhibition mechanisms.

Fluorescence measurements

Cytoplasmic Na^+ binding

Sodium binding to the pump can be easily monitored by the Na^+-induced fluorescence decrease of RH421 because of the electrogenic binding of the third sodium ion to the pump (40). This partial reaction is represented in Scheme 1 by the step $E_1 \leftrightarrow Na_3E_1$. The apparent restriction of the electrogenicity essentially to the third Na^+ originates from the fact that in the physiological pH range 1.5–2 protons are bound to the ion sites of the Na,K-ATPase in the absence of Na^+ and K^+ (38). The studied reaction sequence is therefore $H_xE_1 \rightarrow Na_3E_1$ (with $1.5 \leq x \leq 2$, depending on pH and protein preparation; see below). Fig. 2 B shows that the initial state before Na^+ addition is affected by the addition of CLT. The fluorescence decrease upon addition of CLT indicates that the amount of (positive) charge in the binding sites has been increased and corresponds largely to a condition with two elementary charges in the sites, H_2E_1 or $E_2(H_2)$ (Fig. 2 B).

The subsequent addition of Na^+ up to saturation promotes the transition into state Na_3E_1. Results from corresponding experiments are shown in Fig. 4 A. The titration curves in the absence and presence of up to 25 μM CLT do not differ significantly, and their fit by the Hill equation (Eq. 1) led to a determination of concentration-independent average parameters. The half-saturating Na^+ concentration was 7.3 mM and the Hill coefficient was 1.3 (Fig. 4, B and C). At saturating Na^+ concentrations ($>$ 100 mM) the fluorescence levels merge, and the variation between the different traces are on the order of 5%, in agreement with the CLT-concentration dependent artifacts as shown in Fig. 3. Since, as shown in Fig. 1, the enzyme activity is reduced to ~50% in the presence of 25 μM CLT, and since under the same condition the Na^+-binding kinetics in the titration experiments is unaffected, the inhibition cannot be due to blockage of Na^+ binding.

Cytoplasmic H^+ binding

In the absence of Na^+ and K^+, the binding affinity of the ion-binding sites for protons is high enough that at pH 7.2, ~1.5–1.8 H^+ are bound (38). The experimental variation was caused by different protein preparations, most probably due to the (negatively charged) lipid composition in the membrane fragments. Decreasing pH leads to a more complete saturation of the binding sites with up to 2 H^+, $H_xE_1 \rightarrow H_2E_1 \rightarrow E_2(H_2)$. The titration experiments in the presence and absence of CLT as shown in Fig. 7 revealed that the binding kinetics was not affected by the inhibitor, and that the fluorescence levels at low pH merged in both cases (within the deviations produced by the mentioned artifact at 25 μM CLT). The fluorescence level at low pH and in the absence of CLT has

been assigned to the state with two protons bound, $E_2(H_2)$, and is consistent with that of $E_2(K_2)$ (38). Therefore, this partial reaction corresponds in Scheme 1 A to the sequence $E_1 \leftrightarrow K_2E_1 \leftrightarrow E_2(K_2)$.

In this preparation, the addition of 25 μM CLT caused an initial drop that corresponds to the average binding of about half an elementary charge. The pH-dependent fluorescence changes in the presence of CLT are almost negligible, $\Delta F_{max}/F_0 \approx 3\%$, and support the concept that in a majority of the ion pumps the binding sites are already completely occupied by two protons at pH 7.2. The observed fluorescence level after CLT addition would be in agreement with the assumption that CLT induces a protein modification that leads to a tight binding of two protons so that in the subsequent pH titration only a few fluctuating vacancies in the binding sites are filled.

Extracellular K^+ binding

A second partial reaction that can be well monitored in RH421 experiments by titration experiments is the extracellular K^+ binding (Fig. 5) which is represented in Scheme 1 A preferentially by the reaction sequence, $P-E_2 \leftrightarrow P-E_2K_2 \leftrightarrow E_2(K_2)$. Starting from the $P-E_2$ level, titrations similar to those performed with Na^+ in the E_1 conformation were carried out with KCl. In this case, the half-saturation constant is ~0.3 mM in the absence of CLT, with a Hill coefficient that indicates cooperative K^+ binding (Fig. 5, B and C), in agreement with the literature (45).

In Fig. 2 B it is obvious that addition of 25 μM CLT to the enzyme in state $P-E_2$ causes a drop of the fluorescence level that corresponds to an uptake of (on the average) two elementary charges, either 2 Na^+ or 2 H^+. This indicates that CLT induced a transition into a state with occupied ion-binding sites. In a titration experiment, the fluorescence gradually decreased with CLT concentration with a half-saturation concentration of ~8 μM (data not shown). In the presence of CLT, therefore, the subsequent K^+ titration starts from different conditions, i.e., for ion pumps that are still unmodified by CLT the "normal" K^+ binding occurs. In the CLT-modified pumps the addition of K^+ causes displacement of the ions in the binding sites and allows continuous progress in the pump cycle.

Consequently, in this case CLT affects K^+ binding, as can be seen by significantly modified fitting parameters (Fig. 5, B and C). They show both an apparent decrease of K^+ affinity by more than a factor of 2, and a loss of cooperativity. The higher $K_{0.5}$ values in the presence of CLT can be explained by the assumption that a higher K^+ concentration is necessary to replace the H^+ (or Na^+) ions, which are bound because of the CLT action. The decreased Hill coefficient may be explained by the proposal that the first K^+ displaces other cations that are present in the binding sites.

The fluorescence level at high K^+ is always the same if we assume that the small differences found in the presence of various CLT concentrations are caused by the CLT-induced

artifact discussed above. As mentioned in the framework of the standard experiments (Fig. 2 B), this fluorescence level indicates that most of the ion pumps are accumulated in the ion-occluded conformations. Obviously, the presence of saturating Na^+ and K^+ is able to prevent to some extent the enzyme inhibition by CLT and allows pump turnover. This is reflected also by the residual enzyme activity even at saturating CLT concentrations (Fig. 1). At 25 μM CLT the enzyme activity is reduced to 70% in the Na,K mode. Obviously, K^+ is a stronger antagonist to the CLT action than Na^+, since in the absence of K^+ the enzyme activity is reduced to ~30% at 25 μM CLT (Fig. 1).

Backdoor phosphorylation

In the absence of Na^+, the Na,K-ATPase may be phosphorylated by inorganic phosphate, P_i, which forces the ion pump to run backward through the lower half cycle of the Post-Albers cycle (Scheme 1 A), shifting the steady state from the states in E_1 to P-E_2. In the presence of K^+ alone, the pump is mainly in state $E_2(K_2)$, and the addition of P_i shifts the steady state to P-E_2K_2. Because of the high binding affinity for K^+ in the P-E_2 conformation, no K^+ ions will dissociate. In the absence of K^+, protons will serve as a congener of K^+, and they are bound with a significantly lower affinity to the P-E_2 conformation (38). Therefore, in a buffer of pH 7.2 the P_i-induced reaction sequence will be H_nE_1 ($n < 2$) $\rightarrow$ H_2E_1 $\rightarrow$ $E_2(H_2)$ $\rightarrow$ P-E_2H_2 $\rightarrow$ P-E_2. The last reaction step can be detected by the RH421 method since two positive charges are removed from the binding sites (42). This process leads to a significant increase of the fluorescence (Fig. 6 A, *solid circles*). In the presence of increasing CLT concentrations the P_i-induced fluorescence increase declined, and ceased at a CLT concentration of 20 μM (Fig. 6 A).

The CLT-dependent disappearance of the fluorescence increase may be caused by two different mechanisms. The first one would be an enzyme modification that increases the binding affinity for H^+ so strongly that the reaction step, P-E_2H_2 $\rightarrow$ P-E_2, is kinetically inhibited at pH 7.2. The second mechanism would be an inhibitory interaction of CLT with the protein in state $E_2(H_2)$, which traps the pump in a new state, $E_2^{CLT}(H_2)$, that can no longer be phosphorylated. This "inhibited" state must be reversible, however, since the addition of Na^+ allows a (complete) titration into state Na_3E_1 (Fig. 4 A), and in the presence of Na^+, K^+, and ATP a half-maximum enzyme activity is still found in the presence of 20 μM CLT (Fig. 1). In principle, it is possible that both mechanisms are present. Because in the absence of Na^+ and K^+ addition of 25 μM CLT leads to a fluorescence level that corresponds approximately to a state with 2 H^+ in the binding sites (Figs. 2 B and 7), we prefer the proposal that CLT forms a dead-end complex with the $E_2(H_2)$ conformation of the enzyme. This proposal is represented in Scheme 1 B. We replaced ''H'' by ''X'' to account for the fact that the same inhibitory mechanism may hold also in the presence of K^+.

Electrical measurements

The fluorescence experiments described so far covered a large part of the pump cycle shown in Scheme 1 A. The remaining reaction sequence to be investigated is the Na^+-translocating partial reaction, Na_3E_1 $\rightarrow$ $(Na_3)E_1$-P $\rightarrow$ P-E_2Na_3 $\rightarrow$ P-E_2. Various electrophysiological techniques have been used in the literature (27,43,44,46) to analyze this part of the pump cycle.

The employment of time-resolved techniques is useful to gain information that steady-state fluorescence measurements cannot provide. In particular, performing ATP concentration jumps in the presence of sodium and the absence of potassium ions ensures that only the Na^+-branch of the pump cycle will contribute to the detected currents in the time course of the experiments (27).

When the experiments were performed in the presence of different CLT concentrations, the analysis of the pre-steady-state currents (Fig. 8) showed that the kinetics of the ATP-induced reaction was unaffected by CLT in the concentration range up to 30 μM (*insets b–d*). Only the amount of charge, which is the integral of the measured current, was decreased to 50% of the charge obtained in the absence of CLT (inset a), which indicates that the number of participating ion pumps is reduced with increasing CLT concentrations. This fact is consistent with the proposal that a corresponding amount of sodium pumps is halted in a CLT-bound state that is not part of the pump cycle. The magnitude of the residual transient at 30 μM CLT, and hence a residual transferred charge, is consistent with an incomplete inhibition of pump activity achieved at the same CLT concentration (Fig. 1), which is ~50% in both cases.

It is interesting that CLT has a similar inhibitory effect on the SR Ca-ATPase. In a comparable experiment it reduced the charge movement associated with an ATP-concentration jump in the presence of calcium, and left unaffected the time constants that describe the signal decay (8).

Proposal of a molecular mechanism

In summary, the presented experiments cover all reaction steps around the pump cycle and allow the identification of those steps that are affected by CLT. For a mechanistic explanation, it must be kept in mind that even in the highest applied CLT concentrations 50% of the pump activity was conserved in the physiological pump mode, and the concentration dependence (Fig. 1) indicates that this is approximately a saturation value. With both experimental techniques applied, it could be demonstrated that the kinetics of the pump cycle from state H_2E_1 (corresponding to K_2E_1) via Na_3E_1 to P-E_2 was virtually unaffected by the presence of CLT (Scheme 1 A).

All of the experimental evidence can be explained satisfactorily by introducing a single additional (dead-end) reaction step in the K^+-branch of the classical pump cycle for the Na,K-ATPase, $E_2(X_2)$ $\leftrightarrow$ $E_2^{CLT}(X_2)$ (Scheme 1 B). In detail:

1. Considering the results from the Na^+ titration experiments that were carried out by the fluorescence method (Fig. 4) and those obtained with ATP concentration jumps performed with the SSM technique (Fig. 8), a CLT interaction with the ion pump in the sodium-branch of the enzymatic cycle can be excluded. Hence, the affected steps in the pump cycle have to be confined to the potassium-branch of the Post-Albers cycle.

2. From the investigation of the respective reaction sequences between $P\text{-}E_2$ and E_1, it could be demonstrated by pH titration experiments (Fig. 7) that CLT tends to stabilize the protein in a state with two protons bound, and backdoor phosphorylation (Fig. 6) shows that CLT blocks the enzyme in an $E_2(H_2)$ state. The K^+ titration experiments (Fig. 5) indicated that ion binding to the state $P\text{-}E_2$ and protein dephosphorylation are not prevented, but the presence of CLT has an influence on the apparent half-saturation constant and the Hill coefficient for potassium ions. Both effects are in agreement with a gradual shift toward an ion-bound conformation that is induced by CLT interaction with the protein. In fact, supposing that CLT promotes the formation of a E_2H_2 state, a competition of K^+ ions with protons is induced in the (partially) occupied binding sites when KCl is added to CLT-protein complex. As mentioned above, this explains the apparently lowered K^+ affinity of the pump.

3. The observations that at high CLT concentrations the inhibition of the enzyme activity saturates at 30%, that the Na^+-binding affinity is not significantly affected in the presence of CLT, and that the kinetics of the Na^+-transport is not affected, are a strong indication that the formation of the so-called CLT-inhibited state has to be reversed (rapidly) when the steady state is perturbed by addition of Na^+. The presence of saturating Na^+ allows a complete reversal of the inhibition by quantitative transition into state Na_3E_1 (Fig. 4 *A*).

4. Binding of K^+ to the CLT-inhibited state, $E_2^{CLT}(K_2)$, produces a significantly less stable state than when protons are bound, $E_2^{CLT}(H_2)$. This is reflected by the significantly higher enzyme activity in the Na-K mode compared to the Na^+-only mode (Fig. 1).

5. The apparent increase of affinity for P_i evident in Fig. 6 *B* may be explained by a CLT-induced shift of the steady state in the partial reaction $E_1 \leftrightarrow H_2E_1 \leftrightarrow E_2(H_2) \leftrightarrow E_2^{CLT}(H_2)$ strongly to the right so that, because of the then correspondingly higher concentration of state $E_2(H_2)$, the binding affinity for phosphate is apparently increased. Such an effect has been already demonstrated by shifting the steady state of this partial reaction to the right by a pH decrease in the buffer (42).

For all of these reasons, we propose that CLT may promote the formation of an ion-occluded-CLT-bound conformational E_2 state, $E_2^{CLT}(X_2)$, that acts as a dead end for the cycle. This drug-modified state may be formed only from an ion-occluded E_2 state, e.g., $E_2(X_2)$, belonging to the potassium-branch of the pump cycle (Scheme 1 *B*). The presence of a common CLT-bound ''final'' state is demonstrated also in Fig. 2, where steady-state levels relative to CLT-bound states merge together independently of when the drug was added during a standard experiment.

It is worthwhile to note that so far, we cannot exclude the possibility that a CLT-modified state can also be reached from a different conformational state of the protein during its progress through its pump cycle. Up to now, however, all experimental results can be satisfactorily explained by the presented minimal modification of the whole cycle, and it seems unnecessary to introduce other branched reaction pathways.

It should be noted that the inhibitor-induced confinement into a specific conformation has great relevance with respect to crystallographic studies on membrane proteins. In fact, it is well known that very often the presence of one or even two inhibitors is necessary to achieve diffracting crystal structures of high resolution, as reported for SR Ca-ATPase (47–49).

It is interesting that CLT also favors the E_2 conformation in the case of the SR Ca-ATPase (8), and, as previously noted, this analogy is understandable considering the close structural similarity of the two P-type ATPases. It was recently shown that CLT is also a modulator of another family of membrane proteins, the transient potential receptor calcium channels (13). In this case, CLT shows an affinity in the submicromolar range for some channels. Multidrug resistance proteins (14,15), as well as some calcium-dependent K^+ channels (5,10,12), are also targeted by CLT.

Even if no detailed information about CLT binding regions is available for any of these membrane proteins, it seems very probable that this drug can bind to the external surface of the transmembrane region after its preceding partition into the lipid membrane phase. CLT binding may indirectly affect ion/drug binding and/or transport that involves the inner part of the same transmembrane region.

REFERENCES

1. Sawyer, P. R., R. N. Brogden, R. M. Pinder, T. M. Speight, and G. S. Avery. 1975. Clotrimazole: a review of its antifungal activity and therapeutic efficacy. *Drugs.* 9:424–447.

2. Aktas, H., R. Fluckiger, J. A. Acosta, J. M. Savage, S. S. Palakurthi, and J. A. Halperin. 1998. Depletion of intracellular Ca^{2+} stores, phosphorylation of eIF2 α, and sustained inhibition of translation initiation mediate the anticancer effects of clotrimazole. *Proc. Natl. Acad. Sci. USA.* 95:8280–8285.

3. Benzaquen, L. R., C. Brugnara, H. R. Byers, S. Gattonicelli, and J. A. Halperin. 1995. Clotrimazole inhibits cell-proliferation in-vitro and in-vivo. *Nat. Med.* 1:534–540.

4. Sheets, J. J., J. I. Mason, C. A. Wise, and R. W. Estabrook. 1986. Inhibition of rat liver microsomal cytochrome P-450 steroid hydrox-

ylase reactions by imidazole antimycotic agents. *Biochem. Pharmacol.* 35:487–491.

5. Brugnara, C., B. Gee, C. C. Armsby, S. Kurth, M. Sakamoto, N. Rifai, S. L. Alper, and O. S. Platt. 1996. Therapy with oral clotrimazole induces inhibition of the Gardos channel and reduction of erythrocyte dehydration in patients with sickle cell disease. *J. Clin. Invest.* 97:1227–1234.

6. Georgopapadakou, N. H. 1998. Antifungals: mechanism of action and resistance, established and novel drugs. *Curr. Opin. Microbiol.* 1:547–557.

7. Groll, A. H., A. J. De Lucca, and T. J. Walsh. 1998. Emerging targets for the development of novel antifungal therapeutics. *Trends Microbiol.* 6:117–124.

8. Bartolommei, G., F. Tadini-Buoninsegni, S. M. Hua, M. R. Moncelli, G. Inesi, and R. Guidelli. 2006. Clotrimazole inhibits the Ca^{2+}-ATPase (SERCA) by interfering with Ca^{2+} binding and favoring the E_2 conformation. *J. Biol. Chem.* 281:9547–9551.

9. Snajdrova, L., A. D. Xu, and N. Narayanan. 1998. Clotrimazole, an antimycotic drug, inhibits the sarcoplasmic reticulum calcium pump and contractile function in heart muscle. *J. Biol. Chem.* 273:28032–28039.

10. Alvarez, J., M. Montero, and J. Garciasancho. 1992. High-affinity inhibition of Ca^{2+}-dependent K^+ channels by cytochrome-P-450 inhibitors. *J. Biol. Chem.* 267:11789–11793.

11. Brugnara, C., C. C. Armsby, M. Sakamoto, N. Rifai, S. L. Alper, and O. Platt. 1995. Oral-administration of clotrimazole and blockade of human erythrocyte Ca^{++}-activated K^+ channel—the imidazole ring is not required for inhibitory activity. *J. Pharmacol. Exp. Ther.* 273:266–272.

12. Wu, S. N., H. F. Li, C. R. Jan, and A. Y. Shen. 1999. Inhibition of Ca^{2+}-activated K^+ current by clotrimazole in rat anterior pituitary GH(3) cells. *Neuropharmacology.* 38:979–989.

13. Meseguer, V., Y. Karashima, K. Talavera, D. D'Hoedt, T. Donovan-Rodriguez, F. Viana, B. Nilius, and T. Voets. 2008. Transient receptor potential channels in sensory neurons are targets of the antimycotic agent clotrimazole. *J. Neurosci.* 28:576–586.

14. Golin, J., Z. N. Kon, C. P. Wu, J. Martello, L. Hanson, S. Supernavage, S. V. Ambudkar, and Z. E. Sauna. 2007. Complete inhibition of the Pdr5p multidrug efflux pump ATPase activity by its transport substrate clotrimazole suggests that GTP as well as ATP may be used as an energy source. *Biochemistry.* 46:13109–13119.

15. Klokouzas, A., M. A. Barrand, and S. B. Hladky. 2001. Effects of clotrimazole on transport mediated by multidrug resistance associated protein 1 (MRP1) in human erythrocytes and tumour cells. *Eur. J. Biochem.* 268:6569–6577.

16. Huy, N. T., K. Kamei, T. Yamamoto, Y. Kondo, K. Kanaori, R. Takano, K. Tajima, and S. Hara. 2002. Clotrimazole binds to heme and enhances heme-dependent hemolysis—proposed antimalarial mechanism of clotrimazole. *J. Biol. Chem.* 277:4152–4158.

17. Tiffert, T., H. Ginsburg, M. Krugliak, B. C. Elford, and V. L. Lew. 2000. Potent antimalarial activity of clotrimazole in in vitro cultures of *Plasmodium falciparum*. *Proc. Natl. Acad. Sci. USA.* 97:331–336.

18. Trivedi, V., P. Chand, K. Srivastava, S. K. Puri, P. R. Maulik, and U. Bandyopadhyay. 2005. Clotrimazole inhibits hemoperoxidase of *Plasmodium falciparum* and induces oxidative stress—proposed antimalarial mechanism of clotrimazole. *J. Biol. Chem.* 280:41129–41136.

19. Gemma, S., G. Campiani, S. Butini, G. Kukreja, B. P. Joshi, M. Persico, B. Catalanotti, E. Novellino, E. Fattorusso, V. Nacci, L. Savini, D. Taramelli, N. Basilico, G. Morace, V. Yardley, and C. Fattorusso. 2007. Design and synthesis of potent antimalarial agents based on clotrimazole scaffold: exploring an innovative pharmacophore. *J. Med. Chem.* 50:595–598.

20. Jørgensen, P. L., K. O. Hakansson, and S. J. D. Karlish. 2003. Structure and mechanism of Na,K-ATPase: functional sites and their interactions. *Annu. Rev. Physiol.* 65:817–849.

21. Kaplan, J. H. 2002. Biochemistry of Na,K-ATPase. *Annu. Rev. Biochem.* 71:511–535.

22. Albers, R. W. 1967. Biochemical aspects of active transport. *Annu. Rev. Biochem.* 36:727–756.

23. Post, R. L., C. Hegyvary, and S. Kume. 1972. Activation by adenosine triphosphate in the phosphorylation kinetics of sodium and potassium ion transport adenosine triphosphatase. *J. Biol. Chem.* 247:6530–6540.

24. Morth, J. P., B. P. Pedersen, M. S. Toustrup-Jensen, T. L. M. Sorensen, J. Petersen, J. P. Andersen, B. Vilsen, and P. Nissen. 2007. Crystal structure of the sodium-potassium pump. *Nature.* 450:1043–1049.

25. Apell, H. J. 2003. Structure-function relationship in P-type ATPases—a biophysical approach. *Rev. Physiol. Biochem. Pharmacol.* 150:1–35.

26. Bühler, R., W. Stürmer, H. J. Apell, and P. Läuger. 1991. Charge translocation by the Na,K-Pump. 1. Kinetics of local field changes studied by time-resolved fluorescence measurements. *J. Membr. Biol.* 121:141–161.

27. Pintschovius, J., and K. Fendler. 1999. Charge translocation by the Na^+/K^+-ATPase investigated on solid supported membranes: rapid solution exchange with a new technique. *Biophys. J.* 76:814–826.

28. Tadini-Buoninsegni, F., G. Bartolommei, M. R. Moncelli, and K. Fendler. 2008. Charge transfer in P-type ATPases investigated on planar membranes. *Arch. Biochem. Biophys.* 10.1016/j.abb.2008.02.031.

29. Harmel, N., and H. J. Apell. 2006. Palytoxin-induced effects on partial reactions of the Na,K-ATPase. *J. Gen. Physiol.* 128:103–118.

30. Stimac, R., F. Kerek, and H. J. Apell. 2005. Mechanism of the Na,K-ATPase inhibition by MCS derivatives. *J. Membr. Biol.* 205:89–101.

31. Bartolommei, G., F. Tadini-Buoninsegni, M. R. Moncelli, and R. Guidelli. 2008. Electrogenic steps of the SR Ca-ATPase enzymatic cycle and the effect of curcumin. *Biochim. Biophys. Acta.* 1778:405–413.

32. Tadini-Buoninsegni, F., G. Bartolommei, M. R. Moncelli, D. M. Tal, D. Lewis, and G. Inesi. 2008. Effects of high affinity inhibitors on partial reactions, charge movements and conformational states of the Ca^{2+} transport ATPase (SERCA). *Mol. Pharmacol.* 73:1134–1140.

33. Jørgensen, P. L. 1974. Purification and characterization of (Na^++K^+)-ATPase. III. Purification from the outer medulla of mammalian kindey after selective removal of membrane components by sodium dodecyl-sulphate. *Biochim. Biophys. Acta.* 356:36–52.

34. Apell, H.-J., V. Häring, and M. Roudna. 1990. Na,K-ATPase in artificial lipid vesicles. Comparison of Na,K and Na- only pumping mode. *Biochim. Biophys. Acta.* 1023:81–90.

35. Lanzetta, P. A., L. J. Alvarez, P. S. Reinach, and O. A. Candia. 1979. An improved assay for nanomole amounts of inorganic phosphate. *Anal. Biochem.* 100:95–97.

36. Tadini-Buoninsegni, F., G. Bartolommei, M. R. Moncelli, G. Inesi, and R. Guidelli. 2004. Time-resolved charge translocation by sarcoplasmic reticulum Ca-ATPase measured on a solid supported membrane. *Biophys. J.* 86:3671–3686.

37. Kelety, B., K. Diekert, J. Tobien, N. Watzke, W. Dörner, P. Obrdlik, and K. Fendler. 2006. Transporter assays using solid supported membranes: a novel screening platform for drug discovery. *Assay Drug Dev. Technol.* 4:575–582.

38. Apell, H. J., and A. Diller. 2002. Do H^+ ions obscure electrogenic Na^+ and K^+ binding in the E-1 state of the Na,K-ATPase? *FEBS Lett.* 532:198–202.

39. Stürmer, W., R. Bühler, H. J. Apell, and P. Läuger. 1991. Charge translocation by the Na,K-Pump. 2. Ion binding and release at the extracellular face. *J. Membr. Biol.* 121:163–176.

40. Domaszewicz, W., and H. J. Apell. 1999. Binding of the third Na^+ ion to the cytoplasmic side of the Na,K-ATPase is electrogenic. *FEBS Lett.* 458:241–246.

41. Stürmer, W., and H. J. Apell. 1992. Fluorescence study on cardiac glycoside binding to the Na,K-pump—ouabain binding is associated with movement of electrical charge. *FEBS Lett.* 300:1–4.

42. Apell, H. J., M. Roudna, J. E. T. Corrie, and D. R. Trentham. 1996. Kinetics of the phosphorylation of Na,K-ATPase by inorganic phosphate detected by a fluorescence method. *Biochemistry.* 35:10922–10930.

43. Holmgren, M., J. Wagg, F. Bezanilla, R. F. Rakowski, P. De Weer, and D. C. Gadsby. 2000. Three distinct and sequential steps in the release of sodium ions by the Na^+/K^+-ATPase. *Nature.* 403:898–901.

44. Wuddel, I., and H. J. Apell. 1995. Electrogenicity of the sodium-transport pathway in the Na,K-ATPase probed by charge-pulse experiments. *Biophys. J.* 69:909–921.

45. Bühler, R., and H. J. Apell. 1995. Sequential potassium binding at the extracellular side of the Na,K-pump. *J. Membr. Biol.* 145:165–173.

46. Borlinghaus, R., H. J. Apell, and P. Läuger. 1987. Fast charge translocations associated with partial reactions of the Na,K-pump: I. Current and voltage transients after photochemical release of ATP. *J. Membr. Biol.* 97:161–178.

47. Moncoq, K., C. A. Trieber, and H. S. Young. 2007. The molecular basis for cyclopiazonic acid inhibition of the sarcoplasmic reticulum calcium pump. *J. Biol. Chem.* 282:9748–9757.

48. Obara, K., N. Miyashita, C. Xu, I. Toyoshima, Y. Sugita, G. Inesi, and C. Toyoshima. 2005. Structural role of countertransport revealed in Ca^{2+} pump crystal structure in the absence of Ca^{2+}. *Proc. Natl. Acad. Sci. USA.* 102:14489–14496.

49. Takahashi, M., Y. Kondou, and C. Toyoshima. 2007. Interdomain communication in calcium pump as revealed in the crystal structures with transmembrane inhibitors. *Proc. Natl. Acad. Sci. USA.* 104:5800–5805.